15.
A PAPER-BASED 3D SERS PLATFORM FOR THIRAM SENSING

Viktória Horváth[1], Dániel Megyeri[1], Judit Kopniczky[1], Maher Darwish[1], Zsolt Geretovszky[1], Attila Kohut[1]

[1]*University of Szeged, Physics Institute, Department of Optics and Quantum Electronics, Szeged*

Introduction

Surface-enhanced Raman spectroscopy (SERS) enhances the Raman signal of molecules by factors of 10^2–10^{10} using plasmonic nanostructures, enabling sensitive, selective, and non-destructive detection [1]. While SERS can reach trace and even single-molecule detection, quantitative analysis remains challenging due to substrate variability and analyte adsorption effects [2]. Its major strength lies in portable, *in situ* analysis, especially with the rise of handheld Raman devices and spectral databases. Conventional SERS substrates, typically rigid films with silver or gold nanoparticles (NPs), offer good sensitivity but are costly and limited in sampling flexibility. Research now focuses on flexible, porous supports – like paper – that allow easier integration, broader sampling strategies, and higher surface area for nanoparticle deposition [3]. However, existing fabrication methods often fall short in cost, simplicity, or reproducibility. Spark ablation, a physical, solvent-free NP synthesis method, generates aerosol-phase particles suitable for direct deposition onto porous materials. It enables scalable, tunable, and high-purity NP production [4]. In this study, we explore the use of spark-ablated NPs deposited on filter materials to create flexible 3D SERS substrates. We assess how particle characteristics and support type influence SERS performance, with a focus on detecting thiram, a widely used but strictly regulated fungicide. SERS offers a promising approach for thiram detection, but complex spectra and low signal-to-noise ratios hinder straightforward analysis. To overcome this, we applied a deep learning model – based on the work by Wang *et al.* [5] – to classify thiram concentrations, enhancing detection sensitivity beyond traditional visual methods.

Methods

Nanoparticle Generation and Substrate Fabrication

NPs were synthesized using a spark discharge generator (SDG) equipped with Au, Ag, or AuAg alloy electrodes and operated with N_2 or Ar as carrier gas (7 or 10 L/min). Sparking was maintained at 900 V with frequencies between 500-4000 Hz. The resulting aerosol passed through a tube furnace (up to 900 °C) for particle compaction, and particle size distributions were measured using a scanning mobility particle sizer (SMPS). Aerosol particles were deposited onto 47 mm filters (nylon: 0.2-60 μm pore size, or Whatman paper) housed in a plastic holder. Deposition times (2–20 minutes) were adjusted to ensure consistent particle loading. Substrates were examined via scanning electron microscopy (SEM).

Raman Measurements

Filters were cut into ~5 mm × 5 mm squares for SERS analysis. Substrates were tested using 61 ppm ethanolic rhodamine 6G and methanolic thiram solutions (0.03-240 ppm). Each substrate was drop-coated with 3 μL of analyte and air-dried. SERS spectra were recorded using a 785 nm laser (5-20 mW) and a fiber-coupled Raman probe. Data were collected with a cooled spectrometer using 1 s acquisition time unless stated otherwise.

Results and Discussion

Effect of Experimental Parameters on SERS Substrate Performance

Spark ablation enables precise tuning of NP characteristics and deposition conditions, both of which are crucial for optimizing SERS substrates. We investigated how variables such as material composition, particle size and shape, compaction conditions, and filter properties affect the performance and reproducibility of spark ablation-based SERS platforms.

Nanoparticle Material Composition

We compared SERS substrates fabricated using Ag, Au, and 50:50 Ag-Au alloy NPs. Silver produced the highest initial enhancement but degraded significantly over time. Gold substrates showed excellent long-term stability but lower intensity. Alloyed particles offered a balance: they maintained twice the enhancement of gold and were stable for over a month (Figure 1). Alloy particles were therefore used in all subsequent experiments.

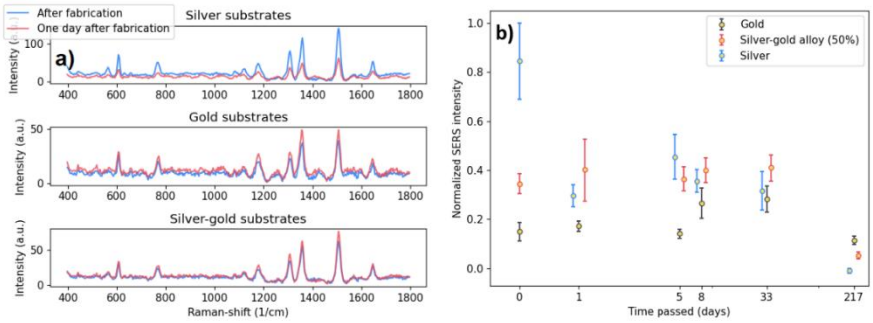

Figure 1. ***a)*** *Stability of SERS substrates fabricated from different NP materials. SERS spectra of rhodamine 6G (R6G) were recorded immediately after fabrication and again one day later.* ***b)*** *Normalized SERS intensities of R6G as a function of time after fabrication for each substrate type.*

Particle Shape and Size

Particle morphology was tuned via spark frequency and furnace compaction temperature. Uncompacted aggregates provided poor enhancement; compaction at ≥300 °C was required for measurable SERS signals, with 800 °C yielding the best performance. This is attributed to improved particle shape and removal of silver oxide layers. Higher spark frequencies yielded larger, broader particle distributions. After heat treatment, particle diameters decreased by 30-46% depending on frequency, with GMD values ranging from ~25-40 nm and GSDs between 1.4-1.6. Substrates produced with compacted particles of ~40 nm GMD and narrow size distributions (GSD <1.56) gave the highest SERS intensities (Figure 2).

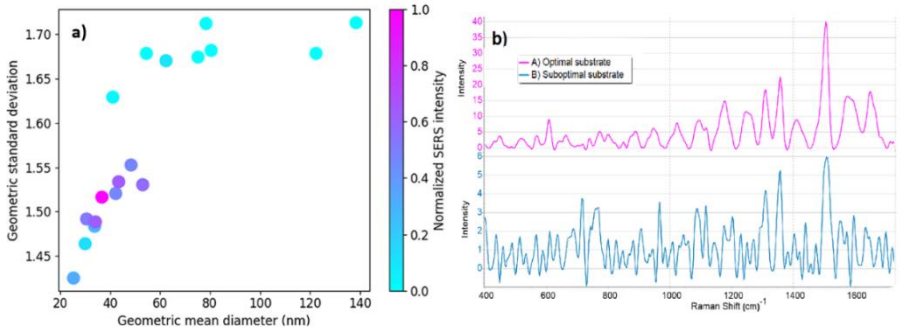

Figure 2. a) Normalized SERS intensities of substrates fabricated from aerosols containing NPs with varying size characteristics. Each point represents a substrate made from particles with a specific geometric mean diameter (GMD) and geometric standard deviation (GSD). Color shading indicates relative SERS intensity.

Pore Size

We tested nylon filters with pore sizes from 0.2 µm to 60 µm. SEM and SERS results showed that smaller pore sizes (0.2-1.2 µm) quickly reached full surface coverage and optimal performance at lower particle loads, while larger-pore filters (10-60 µm) required more material to achieve comparable results. Beyond full coverage, further deposition reduced enhancement due to overloading and loss of surface roughness.

Filter Material

Paper filters were compared to nylon filters of similar pore size (10-11 µm). SEM images revealed that paper filters promote cluster formation in fiber intersections, enhancing plasmonic hotspots. SERS intensity was consistently higher on paper substrates across a range of particle loadings. Additionally, nylon contributed more to the Raman background.

Optimized Substrate and Reproducibility

The optimal SERS substrates were fabricated using Ag-Au alloy particles (3 kHz spark frequency, compacted at 600 °C), deposited on 11 µm pore size paper filters. Maximum enhancement was achieved at a particle loading of 0.8×10^{12} particle number concentration. Substrate-to-substrate reproducibility was good, with a relative intensity deviation of ~23%.

Thiram Detection Using Optimized SERS Substrates

Direct SERS Detection

We tested our substrates with thiram in methanol across a concentration range of 0.03–24 ppm. Strong, distinct peaks (e.g., 1377 cm^{-1}) were visible down to 1.2 ppm, establishing this as the limit of detection (LOD). As shown in Figure 3, in the 2.4–18 ppm range, the signal exhibited a linear response ($R^2 = 0.998$), meeting or exceeding detection needs for most international MRLs. However, below 1.2 ppm, low signal-to-noise ratios and substrate variability limited direct quantification. For rapid screening at lower concentrations, an alternative approach was explored using machine learning.

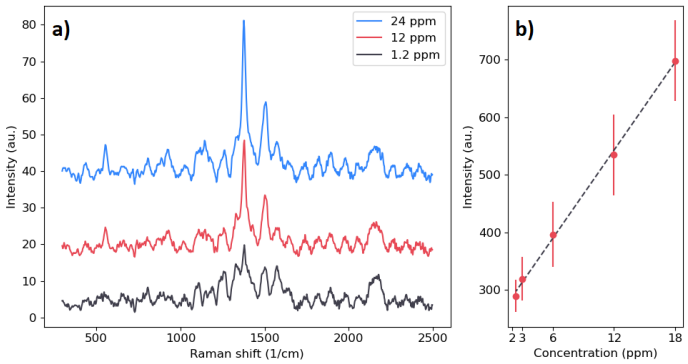

Figure 3. a) SERS spectra of thiram solutions at various concentrations. b) Integrated intensity of the 1377 cm^{-1} peak as a function of thiram concentration.

Deep Learning Classification

A convolutional neural network (CNN), adapted from Wang *et al.* [5], was used to classify thiram spectra into three categories: high (>1.2 ppm), intermediate (0.03-0.48 ppm), and blank (solvent only). The model is illustrated in Figure 4. Trained on 540 spectra, the model achieved 94.4% overall accuracy, with 100% correct classification for both high and blank samples. Misclassifications occurred only in the intermediate range. This method provides rapid, on-site screening with minimal sample preparation. Though not a replacement for gold-standard quantification techniques, combining CNN-based classification with spark-fabricated substrates enables efficient and practical monitoring of thiram contamination in food.

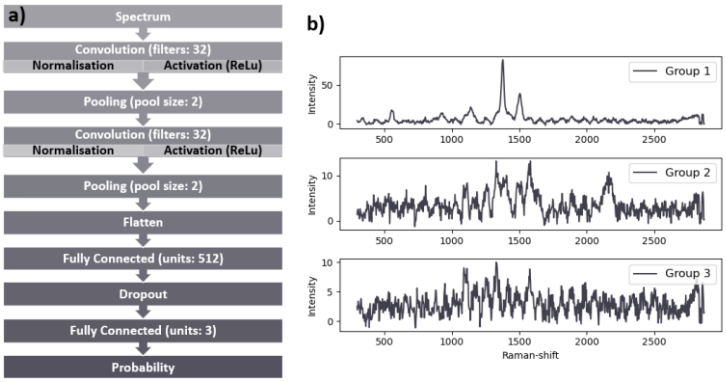

Figure 4. ***a)*** *Architecture of the deep learning model.* ***b)*** *Representative Raman spectra from each category.*

Conclusions

We developed a simple, clean aerosol method to make SERS substrates by spark-ablating alloyed (50 % Ag/50 % Au) electrodes and collecting the resulting nanoparticles on porous filters. By tuning spark frequency and post-deposition heat treatment, we produced compacted particles with log-normal size distributions (GMD 25-138 nm, GSD 1.40-1.71). Optimal SERS performance occurred for GMDs of 30-60 nm and narrow GSDs (1.48-1.56). Filter pore size (0.2-60 μm) had little effect on maximum enhancement – activity could be matched by adjusting loading – but paper filters outperformed nylon, likely due to their organic structure. Using substrates made at 3 kHz and compacted at 800 °C, we detected thiram down to 1.2 ppm directly. A deep-learning model then distinguished three concentration ranges (no thiram, 0.03-0.48 ppm, ≥ 0.48 ppm) with 94 % accuracy, aligning with international maximum-residue limits. This shows that spark-ablation SERS substrates can be mass-produced cheaply, integrated into portable devices, and paired with AI algorithms for rapid sample screening and categorization.

References

[1] Le Ru, E. C.; Blackie, E.; Meyer, M.; Etchegoint, P. G. *Journal of Physical Chemistry C* 2007, **111** (37), 13794–13803.
[2] Pérez-Jiménez, A. I.; Lyu, D.; Lu, Z.; Liu, G.; Ren, B. *Chem Sci* 2020, **11** (18), 4563–4577.
[3] Liu, H.; He, Y.; Cao, K. *Adv Mater Interfaces* 2021, **8** (21), 2100982.
[4] Andreas, Schmidt-Ott, Ed., *Spark Ablation: Building Blocks for Nanotechnology*, Jenny Stanford Publishing, 2020.
[5] Wang, Y.; Fan, X.; Tian, S.; Zhang, H.; Sun, J.; Lu, H.; Zhang, Z. *Chemometrics and Intelligent Laboratory Systems* 2022, **231**, 104657.

Acknowledgments

We are grateful for the funding provided from the National Research, Development and Innovation Fund under the 2022-2.1.1-NL Creation of National Laboratories, Complex Development funding scheme (project 2022-2.1.1-NL-2022-00012), as well as through the EKÖP grant (EKÖP-24-3 - SZTE-511). Research leading to these results has also received funding from the K 146733 (OTKA) project